13

Chemiluminescence-based DNA-Nanomachine with Peroxidase-Like Activity for Detection of Bacterial Nucleic Acids

© P.V. Filatov[1], D.A. Gorbenko[1,2], D.R. Dadadzhanov[1], T.A. Vartanyan[1,¶]

[1] ITMO University,
St. Petersburg, Russia
[2] Molecular Biology and Biotechnology. ITMO University,
St. Petersburg, Russia

¶ e-mail: tavartanyan@itmo.ru

Received October 20, 2025
Revised October 20, 2025
Accepted November 05, 2025

A new chemiluminescence-based system based on a DNA-nanomachine with peroxidase-like activity (PxDm), integrated into a compact closed device, is presented. This system enables the complete workflow — from introduction of the sample under study to obtaining the result. The system was developed for detection of 16S rRNA *Escherichia coli* PxDm demonstrated high versatility and the ability to successfully detect target sequences with high specificity in various sample types: synthetic single-stranded DNA, extracted RNA, and unpurified bacterial lysates. This indicates the system's promise for real-world applications, where samples often contain complex matrix components and preliminary purification is challenging. The system exhibited high selectivity, distinguishing the target microorganism without responding to non-target microorganisms. The ability to work with unpurified samples and without enzymatic steps reduces analysis time and enables integration into point-of-care (POC) express-diagnostic formats. The use of PxDm under such conditions opens new prospects for rapid and accurate monitoring of bacterial infections and food safety control.

Keywords:nucleic acid detection, chemiluminescence, G-quadruplex, DNA-nanomachine, bacterial pathogens.

DOI: 10.61011/EOS.2025.11.62922.8675-25

1. Introduction

The market for diagnostics of bacterial and viral infections, particularly significant amid recent pandemics, is annually valued at tens of billions of dollars [1]. The growing demand for such technologies stems from the need for rapid identification of infectious agents and prevention of dangerous disease outbreaks [2].

Traditional culture-based methods remain the „gold standard" due to their simplicity and low cost [3], yet they require up to a week for results, making rapid response to infection outbreaks impossible [4,5]. Immunochromatographic tests offer portability and ease of use but fall short in sensitivity and are unsuitable for detecting pathogenic mutations, limiting their diagnostic efficacy [6–8]. Nucleic acid amplification-based methods — such as polymerase chain reaction (PCR) and isothermal amplification [9–11] — provide high specificity but require expensive equipment, contamination control, and skilled personnel, hindering their implementation in *point-of-care* (POC) diagnostics [12,13].

Accordingly, there is an increasing demand for rapid, accurate, and highly sensitive methods for detecting bacteria and viruses to safeguard public health [14]. One promising direction is the application of nanotechnologies [15–17], which leverage the unique physicochemical properties of nanomaterials to enhance the efficiency of biosensing systems [18].

DNA nanomaterials have attracted particular attention [19–21], including structures based on G4 — stable, guanine – rich motifs distinguished by high binding affinity and unique catalytic properties [22–26], making them promising as sensing and reporter elements [27,28]. Recent advances in DNA nanotechnology have enabled the creation of PxDm [29,30], capable of highly sensitive detection of bacterial nucleic acids.

Due to the intrinsic catalytic capability of G4 structures that promote luminol oxidation in the presence of hydrogen peroxide [31–33], such systems can generate a detectable luminescent signal (Fig. 1), enabling label-free analyte detection with high sensitivity and reproducibility. PxDm probes, assembled from short oligonucleotides (Fig. S1), operate at ambient temperature without enzymes or prolonged incubation steps, providing improved signal-to-background (S/B) ratios and limits of detection (LOD) compared to linear or split DNA probes.

This study focuses on the development of nanostructured multifunctional probes for rapid nucleic acid sequence analysis at room temperature. Our ultimate goal is to adapt these probes for point-of-care (POC) diagnostic tests, particularly for use in physicians' offices or resource-limited settings without modern laboratory facilities. To achieve this, we employed a chemiluminescent (CL) detection system with a portable, closed-type design featuring a highly sensitive photon counter.

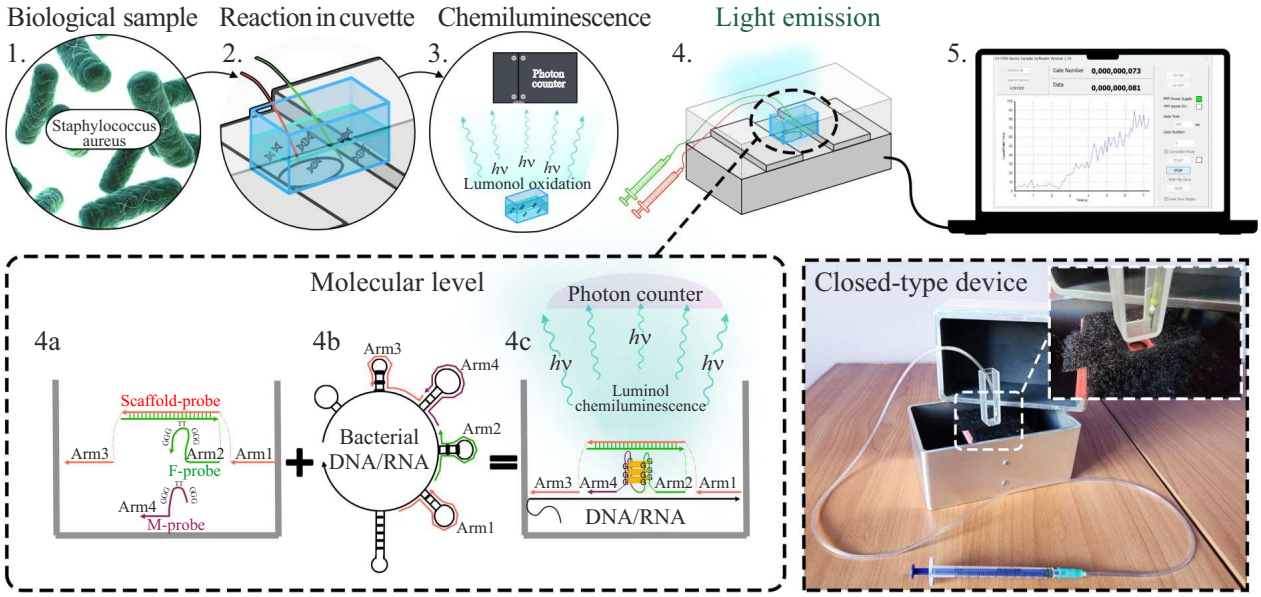

Figure 1. Schematic representation of the target nucleic acid detection method based on luminol chemiluminescence registration. The process involves introduction of the biological sample into the cuvette (1), followed by initiation of the reaction (2), which culminates in photon emission via luminol oxidation (3). At the molecular level (4), the system employs DNA-nanomachine based on G-quadruplex (PxDm) fragments that are initially in a dissociated state (4*a*). Upon introduction of the target nucleic acid (analyte), the PxDm fragments assemble with the analyte, leading to the formation of G-quadruplex structures (G4) (4*b*). These G4 complexes act as catalysts for luminol oxidation, resulting in a rapid chemiluminescent signal (4c). Real-time monitoring of the reaction kinetics (5) enables continuous data collection and analysis via a connected computer, facilitating rapid and sensitive nucleic acid detection.

Previous studies have explored nucleic acid detection based on CL using peroxidase-mimicking DNAzymes and G4-based split DNA probes, achieving nanomolar sensitivity and successful discrimination of single-nucleotide substitutions (SNS) [34–38]. However, factors such as oligonucleotide surface density and preprocessing steps can affect the sensitivity of these systems. To overcome these limitations, we aimed to minimize sample preparation and bioconjugation while reducing diffusion effects through probe design. Additionally, we integrated the entire reaction from sample introduction to signal readout, eliminating the risk of incomplete capture of the luminol oxidation process.

PxDm probes have shown promise in detecting amplification products from complex RNA (based on nucleic acid sequence-based amplification (NASBA)), double-stranded DNA (polymerase chain reaction (PCR)), and differentiating false positives in isothermal amplification methods (LAMP (loop-mediated isothermal amplification) and SPA (stem-loop primer amplification)) [29,30]. Existing studies using G4-based DNA biosensors for bacterial detection have yielded encouraging results. For instance, Du and colleagues developed a G4-based sensor for *Salmonella enterica* detection with a limit of detection of 10 CFU/mL [39]. However, reliance on target-specific antibodies limits its broader application. Similarly, Lee and colleagues reported a G4-based chemiluminescent biosensor for *E. coli* detection with a limit of detection of 100 CFU/mL [40], but it required complex sample preparation and lacked single-nucleotide substitution discrimination capabilities.

In this study, *E. coli* was selected as the model organism—a well-characterized Gram-negative bacterium suitable for RNA detection due to its rapid growth, characteristic gene expression, and high RNA content. Notably, its Gram-negative nature allows 16S rRNA detection without lysozyme, enhancing the method's versatility for point-of-care applications. The chosen microorganism is a common human pathogen, making the method directly applicable for clinical or field diagnostics.

2. Materials and methods

2.1. Oligonucleotides

The oligonucleotides used in this study were custom-synthesized by „Evrogen", Russia. Their sequences are listed in Table S1.

2.2. Bacterial Strains

The *E. coli* K12 strain was selected as the target bacterium for this study. *E. coli* is one of the primary indicator microorganisms in the coliform group, and its detection is critical for assessing fecal contamination of food products. As non-target bacteria, *Listeria monocytogenes* strains,

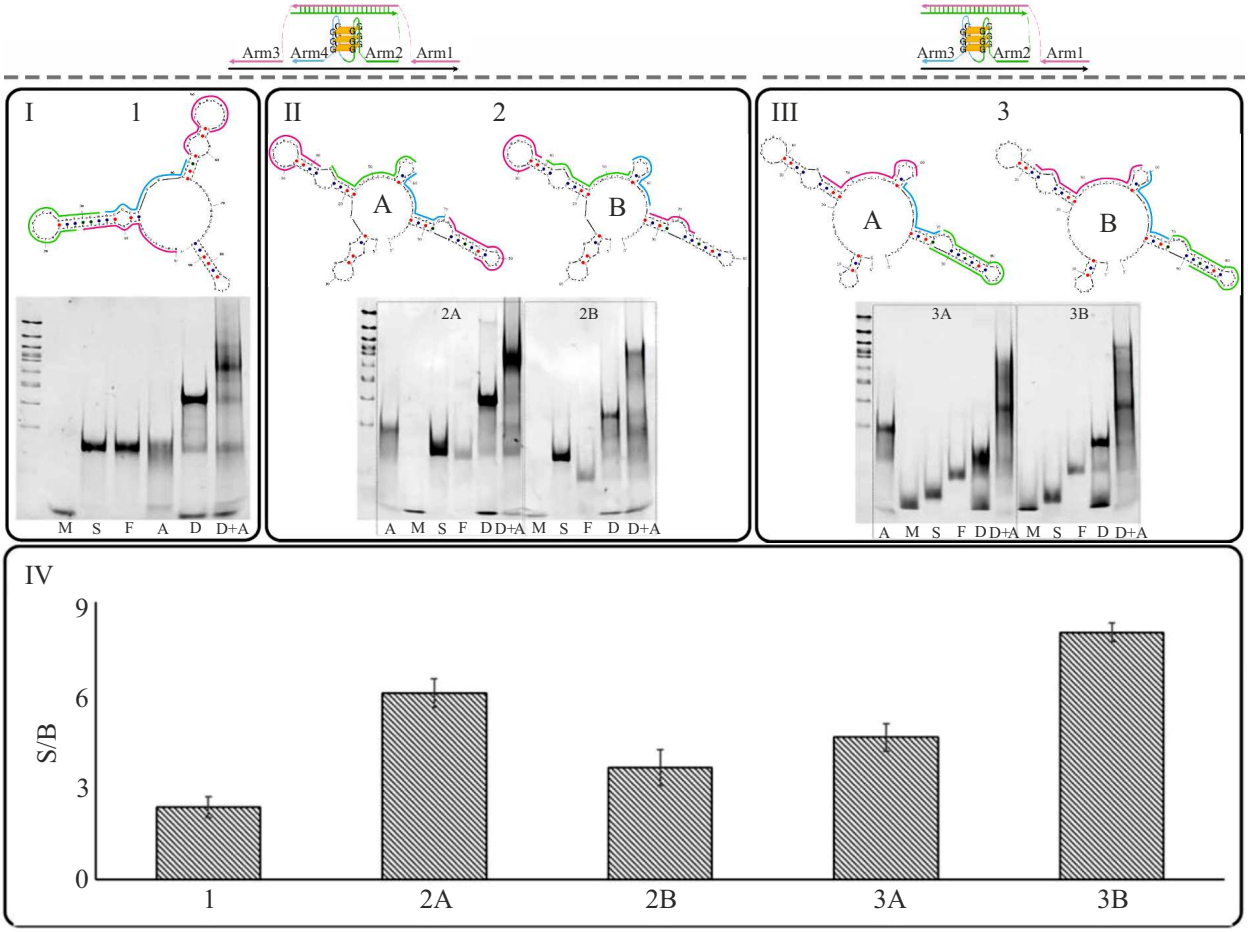

Figure 2. Development and selection of the optimal PxDm design: (I) Demonstration of binding sites for the four-armed PxDm with segment 1 (top panel) and confirmation of construct assembly by 8% native polyacrylamide gel electrophoresis (bottom panel). (II) Similar analysis of four-armed PxDm variants A and B with segment 2 (top and bottom panels). (III) Demonstration of binding sites for three-armed PxDm variants A and B with segment 3 (upper and lower blocks). Probe positions on the gel: M—M-probe, F—F-probe, S — Scaffold-probe; target binding segment (A), PxDm without analyte (D), and PxDm with analyte (D+A). (IV) Calculation of S/B for each PxDm.

kindly provided from the collection of the Research Institute of Children's Infections, St. Petersburg, Russia, were used. All manipulations with live bacteria were performed in designated areas by trained specialists in accordance with Russian Federation regulations.

2.3. Reagents and Equipment

All chemical reagents and equipment used in this study are listed in Table S2.

2.4. Research methods

2.4.1. PxDm Design NCBI databases were used for PxDm design. Target regions of the bacterial genome were identified using the UGENE tool, and the molecular structures of these regions were analyzed with UNAFold and NUPACK. This analysis facilitated the subsequent creation of PxDm adapted to complementary sequences of these regions. The design procedure is described in [29,30].

2.4.2. Polyacrylamide Gel Electrophoresis Native 8% polyacrylamide gel electrophoresis (PAGE) was used to demonstrate successful PxDm assembly. DNA markers of 50 bp and above were used for comparison of oligonucleotide and DNA structure molecular weights. Electrophoresis was then performed for 60 min at 60 V, followed by 30 min at 90 V. The gel was stained with ethidium bromide. Gel visualization was performed using the ChemiDoc imaging system (Bio-Rad).

2.4.3. Agarose Gel Electrophoresis In this study, 2% agarose gel electrophoresis was used to visualize RNA quality. Ethidium bromide was used for gel staining. DNA markers of 100 bp and above were added to control amplicon molecular weight. Electrophoresis was conducted

at 100 V for 30 min. Visualization in gels was performed using the ChemiDoc imaging system (Bio-Rad).

2.4.4. RNA Extraction RNA extraction from *E. coli* and *L. monocytogenes* was performed using Extract RNA solution according to the standard protocol [41].

2.4.5. Chemiluminescent Reaction The reaction mixture consisted of two parts. The first part was used to assemble PxDm and form the G-quadruplex complex. The second part contained the oxidant. Preparation began with the first part. First, 1 μ each of the PxDm scaffold-bearing probes (Scaffold-Probe and F-Probe) were added to COX buffer (35 mM KCl, 60 mM NaCl, 25 mM$MgCl_2$, 25 mM HEPES pH = 7.4, 1% DMSO, 0.03% Triton X-100). The analyte (*E. coli*) was then added. M-Probe was added to a concentration of 250 nM. The reaction mixture was incubated for 10 min at room temperature. Luminol and hemin were added to final concentrations of 10 μM and 1 μM respectively. At the same time, an oxidative mixture was prepared consisting of 1 μM hydrogen peroxide and 5 mM sodium hydroxide dissolved in COX buffer. The first part was transferred to a quartz cuvette for detection using the H11890 photon counter (Hamamatsu, Japan). The oxidative mixture was added prior to detection initiation. After reaction initiation, the total number of photons emitted over 60 s was counted.

2.4.6. Reaction with Cell Lysate Wild-type *E. coli* K12 was cultured in LB medium at 250 rpm and 37°C for 16 h. The overnight culture was washed twice with 0.9% NaCl. Bacterial quantity was estimated based on standard optical density at 600 nm (OD_{600}) for *E. coli* ($2 \cdot 10?$ cells/mL). A CFU test was performed for cell counting. After culture preparation, the lysate was readied for reaction as follows. A sample containing 10^6 cells was centrifuged at 900 g for 5 min. The supernatant was carefully collected, and COX buffer was added to the tube to achieve 10^4 cells. PxDm parts were also added at a final concentration of 1 μM. This mixture underwent annealing, including heating to 95°C for 5 min, followed by cooling to 23°C for 5 min. The mixture was then centrifuged again at 900 g for 5 min. The supernatant from the secondary centrifugation was collected and prepared for the chemiluminescent reaction.

2.4.7. Limit of Detection Determination For LOD calculation, a tube containing only PxDm fragments (Scaffold-Probe 1 mM, F-Probe 1 mM, and M-Probe 250 nM or 1 mM) served to assess background signal from non-specific G-4 formation. The remaining tubes contained target sequences in a range of concentrations.

Linear approximation of the measurement results was then performed, and the limit of detection was determined by the formula

$$\mathrm{LOD} = \frac{3 \times \sigma b}{m}, \quad (1)$$

where σb is the standard deviation of the negative control samples; m is the slope of the linear portion of the signal dependence on concentration.

2.4.8. Selectivity Factor Determination The selectivity factor was chosen as a measure of the diagnostic system's selectivity, indicating the probability of distinguishing the target analyte from non-target ones. The selectivity factor (SF) was determined using the formula below

$$SF = \left(1 - \frac{F_n s - F_0}{F_s - F_0}\right) \times 100\%, \quad (2)$$

where F_0, F_s and F_{ns} are the mean integral intensities calculated from three independent experiments for the specific analyte background signal and non-specific analyte signal, respectively. After reaction initiation, the total number of photons over 60 s was calculated.

2.4.9. Statistical Analysis All experiments were performed at least three times. The Mann-Whitney U-test – was used to determine P values, providing a non-parametric approach to assessing statistical significance. Data in figures are presented as mean ± standard error of the mean, ensuring clear visualization of variability around the means. An P value less than 0.05 was considered indicative of statistically significant differences.

3. Results

3.1. Development and selection of the optimal PxDm

Five PxDm constructs targeting three different regions of the *E. coli* 16S rRNA sequence were designed for detection. Three constructs featured four binding sites for the target fragment (four-armed, Fig. 2: I and II), while two–had three binding sites (three-armed, Fig. 2, III). One construct was developed for segment 1 of *E. coli* 16S rRNA (Fig. 2, I), and two each for segments 2 and 3 (Fig. 2: II and III).

The correct assembly of all PxDm variants was confirmed by 8% native polyacrylamide gel electrophoresis (PAGE). The results demonstrated successful formation of each construct in the presence of the target sequence (Fig. 2: I, II, and III, bottom panel).

Further experiments were conducted both with and without the target sequence (concentration 1 μM). For each construct, the signal-to-background ratio (S/B) was calculated as the target signal (with target sequence) relative to the negative control signal (PxDm only). The obtained values are shown in Fig. 2 IV.

The optimal construct was the three-armed version targeting segment 3 (variant B), which exhibited the highest

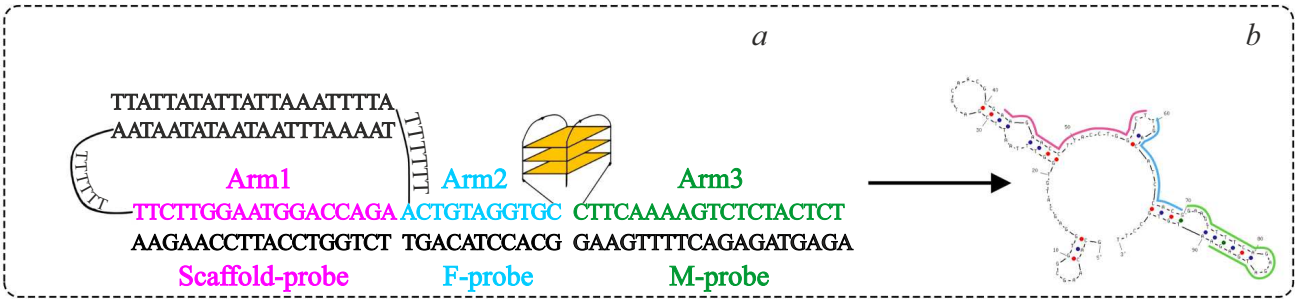

Figure 3. Design of the selected PxDm and secondary structure of the selected target sequence: *a*) PxDm for detection of the *E. coli* 16S rRNA segment, *b*) secondary structure of the *E. coli* 16S rRNA segment.

S/B = 8.0 ± 0.3. This PxDm construct was selected for subsequent experiments.

The molecular configuration and secondary structure of the binding region for the selected three-armed PxDm construct with *E. coli* 16S rRNA are shown in Fig. 3, *a, b.*

3.1.1. Determination of Optimal PxDm Component Ratio After selecting the optimal PxDm, an experiment was conducted to determine the best component ratio. The ratio of M-probe to scaffold-containing probes (F-Probe and Scaffold-Probe) was varied. The optimal ratio was 1 μM scaffold-containing probes to 0.25 μM M-Probe. This combination yielded an S/B of 16.6 ± 0.6 (Fig. S2, B). This ratio was used in all subsequent experiments.

3.2. Determination of Specificity and Limit of Detection

As a primary test of PxDm for *E. coli* 16S rRNA detection, experiments assessing system sensitivity and selectivity were performed using synthetic single-stranded DNA sequences. The limit of detection (LOD), reflecting the minimum target sequence concentration reliably detectable by the system, was first determined. A series of experiments with varying target sequence concentrations was conducted, measuring the Cl signal and constructing a calibration curve (Fig. 4, *a*). The results indicated a LOD of 12 nM.

System selectivity was then evaluated via the selectivity factor (SF). Various sequences were added to the PxDm reaction: target, target with single-nucleotide substitutions (SNS 1.1, SNS 1.2, SNS 1.3), and a non-target sequence from the *L. monocytogenes* genome (Fig. 4, *b*). The calculated SF values for non-target sequences were 59%, 51%, 71%, and 86%, respectively, indicating sufficient system specificity to distinguish the target sequence from closely related and non-target analogs.

3.3. Detection of Extracted RNA and Cell Lysate

After demonstrating PxDm efficacy with synthetic analytes, its applicability under near-real conditions was confirmed using extracted *E. coli* RNA and unpurified bacterial lysate.

In the first stage, PxDm detection was performed with extracted *E. coli* RNA at 300 ng/μL obtained from a liquid bacterial culture at 10,000 cells/mL. RNA extraction was done by standard methods, with integrity and purity confirmed by 2% agarose gel electrophoresis (Fig. S3). For specificity validation, RNA from the non-target bacterium *L. monocytogenes* at the same concentration was used (Fig. 5, *a*). The results showed no PxDm assembly in the presence of non-target RNA, as evidenced by a Cl signal comparable to the negative control. The target reaction signal ratio to negative control was 1.7 ± 0.1 ($p < 0.05$), whereas for the non-target sequence it was 2.2 ± 0.4 ($p < 0.01$).

After confirming efficacy in RNA-based tests, experiments detecting *E. coli* lysate were conducted (Fig. 5, *b*). Lysate from a bacterial culture at 10,000 cells/mL, matching the RNA experiment conditions, was analyzed. The procedure followed sections 2.4.6–2.4.9and Appendix 4. The data showed that the target lysate reaction signal statistically significantly exceeded the negative control by 1.8 ± 0.2 fold ($p < 0.05$).

Comparison of S/B values revealed their comparability for both sample types: 1.7 for the RNA reaction and 1.8 for the lysate. Thus, PxDm maintains stable specificity and sensitivity when working with both purified nucleic acids and real biological samples.

4. Discussion

This study presents results on the creation, optimization, and characterization of a CL PxDm for detecting bacterial nucleic acids, targeting a *E. coli* 16S rRNA segment. Five constructs were developed for three different target regions, with the three-armed sensor construct providing the highest S/B = 8.0 ± 0.3. It was shown that increasing the number of binding sites in the construct does not necessarily enhance efficiency when working with single-stranded sequences, even accounting for their secondary structures. Optimization of

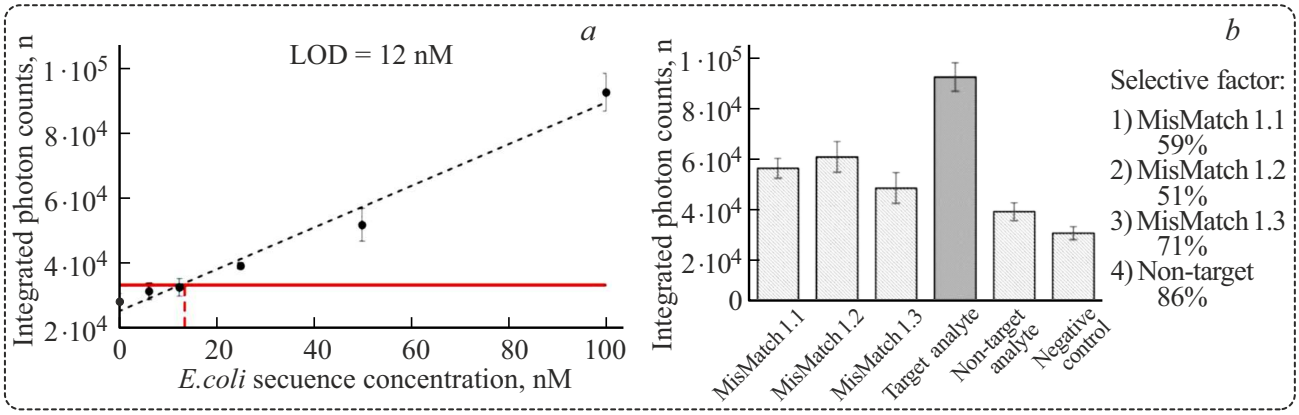

Figure 4. Determination of PxDm construct sensitivity and specificity for synthetic single-stranded DNA analytes. Integral photon counts were used to construct calibration curves and subsequent LOD (*a*) and SF (*b*) determination.

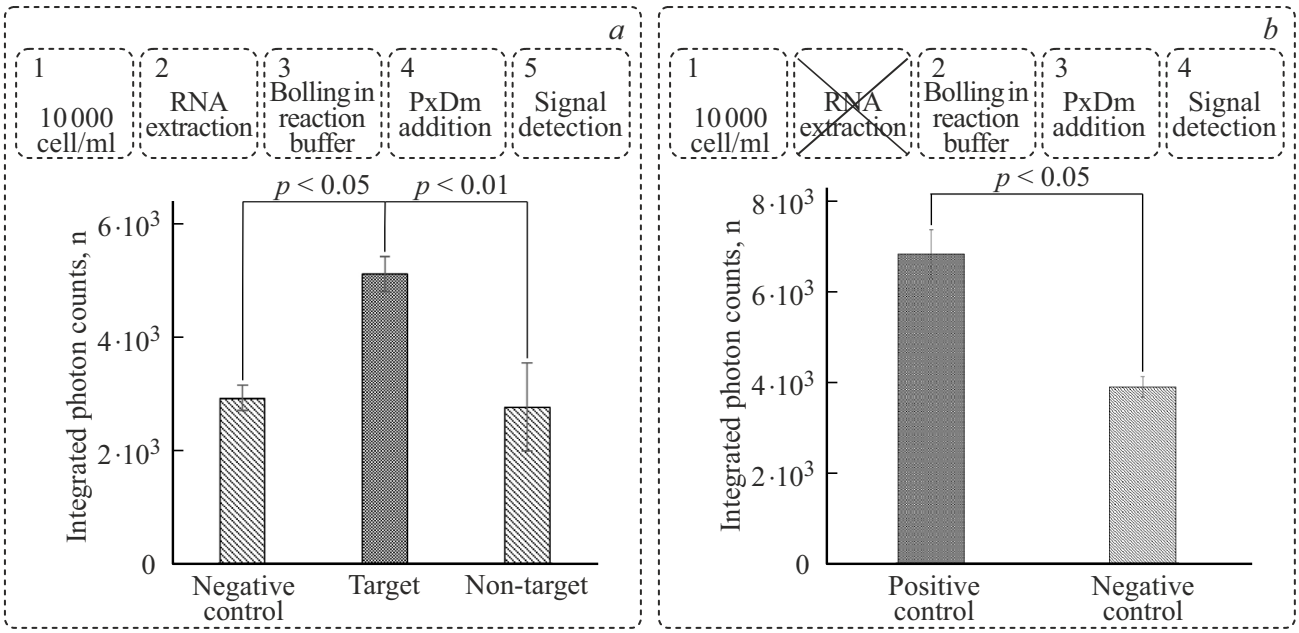

Figure 5. Detection of extracted RNA and *E. coli* cell lysate using PxDm. (1) Total photon emission values obtained in reactions with isolated RNA from *E. coli* (target) and *L. monocytogenes* (non-target), both at 300 ng/μL. Negative control lacks the analyte sequence. (2) Total photon emission values obtained in reactions with cell lysate. Positive control represents PxDm reaction with cell lysate in COX buffer at 10,000 cells/mL. Negative control represents PxDm reaction without analyte in buffer.

the PxDm component ratio further increased the S/B to 16.6 ± 0.6.

The PxDm for *E. coli* detection demonstrated a limit of detection (LOD) of 12 nM and 86% specificity relative to non-target microorganisms. The system detected single-nucleotide substitutions with a selectivity factor up to 71%, confirming its high specificity. Successful detection of both extracted *E. coli* RNA and cell lysate demonstrates the applicability of this platform to real analytical tasks.

However, the PxDm system's detection limits remain relatively high for some categories of biological samples, particularly genomic DNA. A promising direction to address this could involve modifying the DNA construct design by incorporating additional G4 sequences to amplify the detection signal. Regarding system specificity, it could be enhanced by optimizing the M-probe length—shortening the hybridization region may increase selectivity for target analytes. Shorter probe arms reduce the likelihood of stable intramolecular structure formation and non-specific binding to extraneous nucleic acids present in the sample. Concurrently, achieving nucleic acid detection without prior amplification requires further increasing the signal-to-background ratio (S/B) by reducing background signal, which was one of the key objectives for future research.

Notably, the concept of using split G4-based CL sensors for detection is not novel, as demonstrated by colleagues in 2021 [42]. A chemiluminescent sensor based on the G4/hemin complex formed during B-actin amplification achieved high sensitivity (LOD = 3.8 fM) surpassing PxDm. However, it relies on PCR amplification products, requiring expensive thermocyclers and limiting its use for single-nucleotide substitution detection. In contrast, the PxDm system offers advantages such as minimal sample preparation, no prior amplification, and high specificity for single-nucleotide substitution recognition. These features expand PxDm applicability compared to amplification-based methods, positioning it as a promising complement to existing nucleic acid detection strategies and broadening the potential of G4-based chemiluminescent systems. Moreover, our study introduces a unique closed-system design, rendering the potential device suitable for POC applications.

5. Conclusions

This study successfully developed and characterized a CL PxDm for rapid and specific detection of *E. coli* 16S rRNA. The PxDm system demonstrated a single-stranded *E. coli* DNA LOD of 12 nM with 86% specificity toward non-target microorganisms. The PxDm system is capable of detecting extracted RNA even in complex biological samples. RNA was detected at 300 ng/μL, and cell lysate was analyzed using PxDm at 10? cell/mL. The obtained results confirm the promise of the PxDm method for point-of-care (POC) diagnostic systems. The study demonstrates the substantial potential of the PxDm platform as an innovative tool for developing highly efficient pathogen detection diagnostic systems, contributing to advancements in clinical diagnostics and infectious disease monitoring methods.

Acknowledgments

Special thanks to Dr. Natalia Virts, Maria Rubel, and Maria Berezovskaya for fruitful ideas and productive discussions. The authors would like to thank the Research Institute of Children's Infections for work with bacterial strains. The authors thank Dr. Dmitry Kolpashchikov for inspiration and moral support.

Funding

The study was supported by the Russian Science Foundation grant № 23-72-00045, https://rscf.ru/project/23-72-00045/

Conflict of interest

The authors declare that they have no conflict of interest.

Equipment

The following instruments were used in the study: NanoPhotometer N50 (Implen, Germany), water bath LB-140 (LOIP, Russia), mini-centrifuge/vortex FV-2400 (Biosan, Latvia). Additional equipment included a flask heater LH-125 (LOIP, Russia), centrifuge 5418 R (Eppendorf, Germany), vertical electrophoresis cell Mini-PROTEAN Tetra (Bio-Rad, USA), gel imaging system ChemiDoc? Touch Gel (Bio-Rad, USA), and photon counter H11890 (Hamamatsu, Japan).

Annex 1

Oligonucleotides, reagents, and equipment used in this study, Tables S1, S2.

Table S1. Oligonucleotides used in this study

Oligo	Sequence 5′–3′
E. coli	GCACAAGCGGTGGAGCATGTGGTTTAATTCGATGCAACGCGAAGAACCTTACCTGGTCTT GACATCCACGGAAGTTTTCAGAGATGAGAATGTGCCTT
E. coli M-probe	TCTCATCTCTGAAAACTTCTTTTTTACCGGGTTGGG
E. coli	F-probe GGGTTGGGACCTTTTTTCGTGGATGTCATTTTTTATTTTAAATTATTATATTATT
E. coli Scaffold-probe	AGACCAGGTAAGGTTCTTTTTTTTAATAATATAATAATTTAAAAT
E. coli MisMatch	GCACAAGCGGTGGAGCATGTGGTTTAATTCGATGCAACGCGAAGAACCTT ACCTGGTCTTGACATCCACGGAAGTTTTCAGAGATAAGAATGTGCCTT
H. influenzae	AATTCTACCCCTCCCTAAAGTACTCTAGTTACCCAGTCTGAAATGCAATT CCTAGGTTAAGCCCAGGGCTTTCACACCTCACTTAAATAACC
L. monocytogenes	ATGAAAAAAATAATGCTAGTTTTTATTACACTTATATTAGTTAGTCTACC AATTGCGCAACAAACTGAAGCAAAGGATGCATCTGCATTCAATAAAGAAAATTCAATTTCATCCATGGCA CCACCAGCATCTCCGCCTGC

Table S2. Reagents used in this study

Reagent	Supplier	Country	Purpose
Oligonucleotides	Evrogen	Russia	PxDm
Nuclease-free water	Cyagen	USA	Oligonucleotide dilution
4-(2-Hydroxyethyl)-1-piperazineethanesulfonic acid (HEPES)	Molecule	Germany	Buffer preparation
Potassium chloride (KCl)	Carl Roth	Germany	Buffer preparation
Magnesium chloride (MgCl?)	Helicon	Russia	Buffer preparation
Sodium chloride (NaCl)	Vekton	Russia	Buffer preparation
Triton X-100	Sigma-Aldrich	USA	Buffer preparation
DMSO	AppliChem	Germany	Buffer preparation
Tris(hydroxymethyl) aminomethane hydrochloride	Amresco	USA	TBE buffer preparation
Boric acid	Helicon	Russia	TBE buffer preparation
Ethylenediaminetetraacetic acid (EDTA)	Helicon	Russia	TBE buffer preparation
Acrylamide	AppliChem	Germany	PAGE gel electrophoresis components
N, N'-Methylenebis- - acrylamide components	Helicon	Russia	PAGE gel electrophoresis PAGE
Ammonium persulfate components	Helicon	Russia	PAGE gel electrophoresis PAGE
TEMED (N,N,N',N'-tetramethylethylenediamine components	Molecule	Germany	PAGE gel electrophoresis PAGE
Reagent	Supplier	Country	Purpose
Agarose	Dia-M	Russia	Agarose gel electrophoresis component
Ethidium bromide	Amresco	USA	Gel electrophoresis staining
100 bp+DNA ladder	Evrogen	Russia	Nucleic acid length determination by gel electrophoresis
4x Gel loading dye	Evrogen	Russia	Sample loading for gel electrophoresis
Phenol	Vekton	Russia	RNA extraction
Chloroform	Acros Organic	Russia	RNA extraction
Isopropanol	Vekton	Russia	RNA extraction
ExtractRNA	Evrogen	Russia	RNA extraction
Hemin	Sigma-Aldrich	USA	Chemiluminescent reaction
Luminol	Sigma-Aldrich	USA	Chemiluminescent reaction
H_2O_2 30%	AppliChem	Germany	Chemiluminescent reaction
NaOH	Sigma-Aldrich	USA	Chemiluminescent reaction

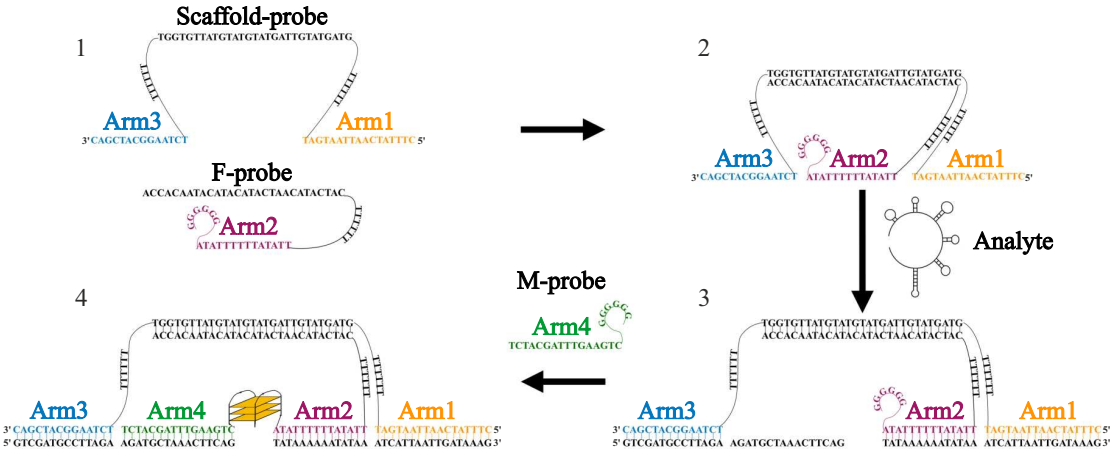

Fig. 1S. Schematic representation of PxDm assembly as an example construct for 16S rRNA *E. coli* detection: *1* — assembly of scaffold-containing probes in reaction buffer (Scaffold-Probe and F-Probe), *2* — addition of target analyte, *3* — addition of short probe carrying the G4 portion (M-Probe), *4* — fully assembled construct.

Annex 2

PxDm Design and Assembly

The assembly scheme for the three-armed PxDm is shown in Fig. S1.

The system consists of three oligonucleotides: Scaffold-Probe, F-Probe and M-Probe (Table S1). Each probe includes various segments — arm 1, arm 2, arm 3, and arm 4 —complementary to specific regions of the target sequence (analyte). Each part performs its function. The Scaffold-Probe plays a key role in stabilizing the entire system. It includes a segment complementary to the analyte and another segment non-complementary to the analyte, thus forming a scaffold with the F-Probe. The F-Probe is necessary for the overall system affinity. In addition to the scaffold and analyte-complementary site, this probe also contains half of the split G4 structure. The M-Probe, on the other hand, contains the other half of the G4 and plays a key role in system selectivity. Thus, in the presence of the target analyte, the two G4 halves unite, forming a complete reactive G4 that serves as the signaling component of PxDm.

Appendix 3

PxDm Composition Optimization

To optimize the chemiluminescent signal, a series of reactions was conducted using the selected PxDm with various molar ratios of M-Probe to scaffold-containing probes (Scaffold-Probe and F-Probe) in the reaction mixture. The following molar ratios of scaffold-bearing probe to M-Probe were evaluated: 1) 1 : 1, 2) 1 : 0.25 and 3) 0.25 : 1 μM respectively. For the PxDm intended for 16S rRNA *E. coli* region detection, composition 2 demonstrated the optimal S/B ratio of 16.6 $\pm$ 0.6, and was selected for further studies. A comparison of the obtained values is presented in Fig. S3.

Appendix 4

Extracted RNA Detection

The sample was first homogenized in Extract RNA solution (overnight culture centrifuged at3000–5000 g for 2 min). Culture liquid was removed, and the pellet was re-suspended in 1 mL Extract RNA. The lysate was incubated at 50°C for 10 min, then centrifuged at 12 000–15 000 g for 10 min to remove insoluble fragments. The supernatant was transferred to a new tube. 200 μL of chloroform:isoamyl alcohol mixture (ratio24 : 1was added to the supernatant. The tube contents were vigorously mixed by manual shaking for 15 s. The resulting mixture was incubated for 3–5 min at room temperature with periodic shaking. The sample was then centrifuged at 12,000 g for 15 min at 4°C. The aqueous phase (upper) was transferred to a new tube, avoiding the interphase. Then, 1/2 volume of RNA extract and 1/5 volume of chloroform with isoamyl alcohol were added. The sample was centrifuged at 12,000 g for 15 min at 4°C. The upper phase was collected into a new

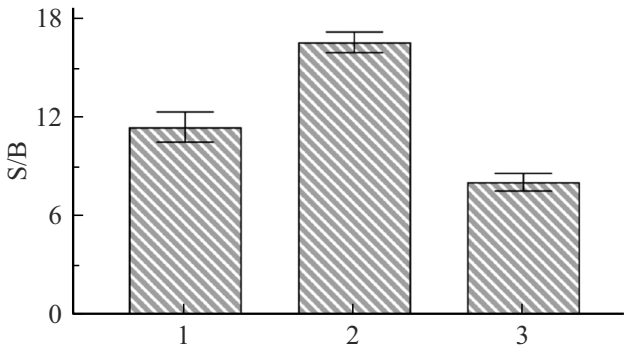

Fig. 2S. Optimization of PxDm component ratios for 16S rRNA *E. coli* detection. Target reaction signal-to-negative control ratios for each probe composition for the developed PxDm (*1*–*3*) with standard error.

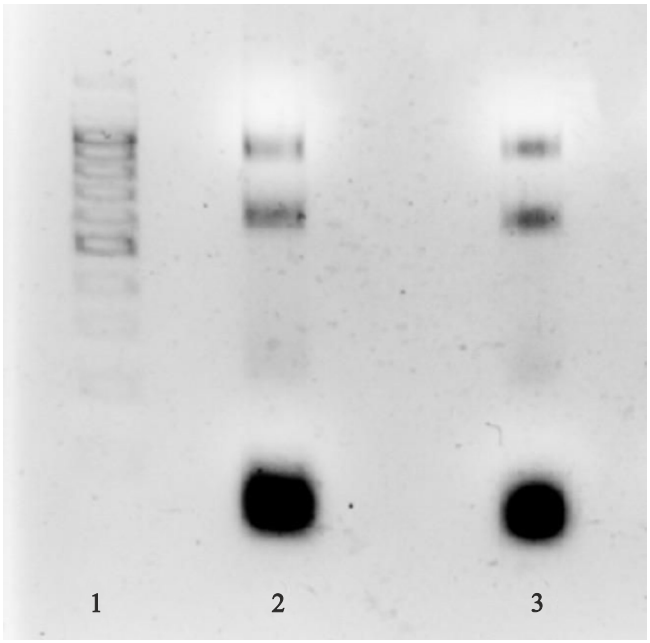

Fig. 3S. Visualization of extracted RNA in 2% agarose gel: *1* — 100+ bp DNA, *2* — isolated *E. coli* RNA, *3* — isolated *L. monocytogenes* RNA.

Eppendorf tube. Subsequently, 500 μL isopropanol was added for RNA precipitation. The mixture was incubated at room temperature for 10−15 min. After incubation, the sample was centrifuged at 12,000 g for 10 min at room temperature. The supernatant was discarded, leaving the RNA pellet at the bottom of the tube. Then, 1 mL of 80% ethanol was added. The sample was centrifuged at maximum speed for 5 min at room temperature. Ethanol was removed. The pellet was air-dried in the open tube for 5−7 min. The RNA was then dissolved in the required volume of RNase-free water. RNA quality was confirmed by 2% agarose gel electrophoresis, as shown in Fig. S3.

References

[1] Bacterial and Viral Specimen Collection Market Size. Global Market Insights, 2024. [Electronic source]. URL: https://www.gminsights.com/industry-analysis/bacterial-and-viral-specimen-collection-market (Date of access: 19.10.2025).

[2] H. Harpaldas, S. Arumugam, C.C. Rodriguez, B.A. Kumar, V. Shi, S.K. Sia. Lab Chip, **21** (23), 4517 (2021). DOI: 10.1039/d1lc00627d

[3] A.M. Alizadeh, R.K. Movahed, M. Mohammadnia. Tanaffos, **15** (2), 112 (2016). https://pubmed.ncbi.nlm.nih.gov/27904544/

[4] P. Maffezzoli, M. Kestler, A. Burillo, S. Corcione, F.G. De Rosa, P. Muñoz, E. Bouza. Rev. Esp. Quimioter., **38** (1), 8 (2025). DOI: 10.37201/req/094.2024

[5] N. Navvabi, L. Pérez-Rodríguez, M. Del Villar-García, J. Ramírez-Salinas, F. Munõz-Valle. Rev. Gastroenterol. Mex. Engl. Ed., **87** (2), 176 (2022). DOI: 10.1016/j.rgmxen.2021.11.007

[6] S. Rodríguez de Córdoba, A. Reparaz, D. Sanchez, S. Pinto, L.J. Lopez, H.M. Merinero, I. Calvete, J. Perez-Perez, S.S. Jellison, Y. Zhang, R.J.H. Smith, I. Moreno, M. Dominguez. Front. Immunol., **15**, 1527016 (2025). DOI: 10.3389/fimmu.2024.1527016

[7] MyBioSource Editorial Team. Comparison of PCR with Other Nucleic Acid Amplification Techniques. MyBioSource [Electronic source]. URL: https://www.mybiosource.com/learn/comparison-of-pcr-with-other-nucleic-acid-amplification-techniques/ (Date of access: 19.10.2025).

[8] T. Notomi, H. Okayama, H. Masubuchi, T. Yonekawa, K. Watanabe, N. Amino, T. Hase. Nucleic Acids Res., **28** (12), e63 (2000). DOI: 10.1093/nar/28.12.e63

[9] S. Rentschler, L. Kaiser, H.P. Deigner. Int. J. Mol. Sci., **22** (1), 456 (2021). DOI: 10.3390/ijms22010456

[10] V. Iyer, A. Smith, J. Doe, M. Lee, R. Kumar. J. Clin. Microbiol., **62** (3), e01498-23 (2024). DOI: 10.1128/JCM.01498-23

[11] G.V. Guedez-Ló pez, M. Alguacil-Guillé n, P. Gonzá lez-Donapetry, A. et al. Eur. J. Clin. Microbiol. Infect. Dis., **39** (10), 2289 (2020). DOI: 10.1007/s10096-020-04010-7

[12] M. Fakruddin, M. Zinnat, S. Hossain, A. Kamal, M. Islam. J. Pharm. Bioallied Sci., **5** (4), 245 (2013). DOI: 10.4103/0975-7406.120066

[13] M. Anahtar, G. McGrath, B. Rabe, N. Tanner, B. White, J. Lennerz, J. Branda, C. Cepko, E. Rosenberg. Open Forum Infectious Diseases, **8** (2), ofaa631 (2021). DOI: 10.1093/ofid/ofaa631

[14] H. Lahiri, K.S. Basu. Biosensors, **15** (3), 130 (2025). DOI: 10.3390/bios15030130

[15] K.Z. Chng, Y. Wu, X. Zhang, T. Li, Y. Yang, L. Zhang. Sens. Actuators B Chem., **339**, 129849 (2021). DOI: 10.1016/j.snb.2021.129849

[16] H.K. Choi, J. Yoon. Biosensors, **13** (2), 208 (2023). DOI: 10.3390/bios13020208

[17] B.D. Malhotra, M.A. Ali. Nanomaterials for Biosensors. In: Micro and Nano Technologies, William Andrew Publishing, 1−74 (2018). DOI: 10.1016/B978-0-323-44923-6.00001-7

[18] U. Gurkan, S. Moon, H. Geckil, F. Xu, S. Wang, T. Lu, U. Demirci. Biotechnol J., **6** (2), 138−149 (2011). DOI: 10.1002/biot.201000427

[19] E.E. Iwaniuk, T. Adebayo, S. Coleman, C.G. Villaros, I.V. Nesterova. Nucleic Acids Res., **51** (4), 1600 (2023). DOI: 10.1093/nar/gkad031

[20] J. Dong, M.P. O'Hagan, I. Willner. Chem. Soc. Rev., **51** (17), 7631 (2022). DOI: 10.1039/D2CS00317A

[21] C. Luo, X. Li, Y. Li. Int. J. Nanomedicine, **19**, 441 (2024). DOI: 10.2147/IJN.S442335

[22] D. Calabria, A. Pace, E. Lazzarini, I. Trozzi, M. Zangheri, M. Guardigli, S. Pieraccini, S. Masiero, M. Mirasoli. Biosensors, **13**, 650 (2023). DOI: 10.3390/bios13060650

[23] A. Sarwar, B. Chen, C. Li, D. Wang, E. Patel. Int. J. Biol. Macromol., **223**, 147825 (2025). DOI: 10.1016/j.ijbiomac.2025.147825

[24] H. Yang, Y. Zhou, J. Liu. Trends Anal. Chem., **132**, 116060 (2020). DOI: 10.1016/j.trac.2020.116060

[25] M. Marzano, M.G. Nolli, A.P. Falanga, G. D'Errico, S. Neri. RSC Adv., **15** (23), 17933 (2025). DOI: 10.1039/D5RA01033K
[26] L. Zhang, H. Wang, X. Qu. Adv. Mater., e2211147 (2023). DOI: 10.1002/adma.202211147
[27] Y. Wang, X. Li, Z. Zhang, W. Xu, H. Xiong. Sens. Actuators B Chem., **298**, 126867 (2019). DOI: 10.1016/j.snb.2019.126867
[28] S. Kido, N. Takahashi, H. Miyazaki, S. Kono, K. Saito, A. Kuzuya. ACS Omega, **10** (37), 43300 (2025). DOI: 10.1021/acsomega.5c08498
[29] D.A. Gorbenko, L.A. Shkodenko, M.S. Rubel, A.V. Slyta, E.V. Nikitina, E.A. Martens, D.M. Kolpashchikov. Chem. Commun., **58** (35), 5395 (2022). DOI: 10.1039/d2cc00325b
[30] Y.I. Maltzeva, D.A. Gorbenko, E.V. Nikitina, M.S. Rubel, D.M. Kolpashchikov. Int. J. Mol. Sci., **24** (9), 7812 (2023). DOI: 10.3390/ijms24097812
[31] Q. Zhu, D. Tian, W. Guo, J. He. Anal. Lett., **55**(8), 1179–1191 (2021). DOI: 10.1080/00032719.2021.1991365
[32] K. Tsukakoshi, H. Abe, H. Ikebukuro, K. Karube. Nucleic Acids Res., **49** (11), 6069 (2021). DOI: 10.1093/nar/gkab388
[33] P. Qi, Z. Sun, Y. Huang, X. Feng, L. Zhang. Colloids Surf. A Physicochem. Eng. Asp., **655**, 130319 (2022). DOI: 10.1016/j.colsurfa.2022.130319
[34] P. Zou, J. Cao, Y. Xu, L. Du. Biosens. Bioelectron., **79**, 29 (2016). DOI: 10.1016/j.bios.2015.12.012
[35] Y. Gao, B. Li. Anal. Chem., **85** (23), 11494 (2013). DOI: 10.1021/ac402728d
[36] Y. Guan, X. Li, H. Wang, Z. Zhang, J. Li. Biosensors, **13** (1), 118 (2023). DOI: 10.3390/bios13010118
[37] V. Pavlov et al. Anal. Chem., **76** (7), 2152 (2004). DOI: 10.1021/ac035219l
[38] S. Bi, S. Yue, S. Zhang. Chem. Soc. Rev., **46** (14), 4281 (2017). DOI: 10.1039/C7CS00055C
[39] R. Du, X. Yang, P. Jin, Y. Guo, H. Cheng, H. Yu, Y. Xie, H. Qian, W. Yao. Crit. Rev. Food Sci. Nutr., **63** (27), 8808 (2023). DOI: 10.1080/10408398.2022.2059753
[40] E.M. Gross, S.S. Maddipati, S.M. Snyder. Bioanalysis, **8** (19), 2071 (2016). DOI: 10.4155/bio-2016-0178
[41] Biosearch Technologies. QuickExtract RNA Extraction Kit Protocol [Electronic source]. URL: https://www.biosearchtech.com/nucleic-acid-sample-preparation/rapid-nucleic-acid-extraction-kits/quickextract-rna-extraction-kit/p/QER090150 (Date of access: 19.10.2025).
[42] H. Ying, S. Fengying, H. Feng, W. Yanhong, X. Xianru, X. Xiaolei. Transl. Oncol., **14** (1), 100928 (2021). DOI: 10.1016/j.tranon.2020.100928

Translated by J.Savelyeva